Available online at www.sciencedirect.com
ScienceDirect
Journal of Power Sources 172 (2007) 659–665
JOURNAL OF POWER SOURCES
www.elsevier.com/locate/jpowsour

Factors affecting methanol transport in a passive DMFC employing a porous carbon plate

Mohammad Ali Abdelkareem, Nobuto Morohashi, Nobuyoshi Nakagawa *

Department of Biological and Chemical Engineering, Gunma University, 1-5-1 Tenjin, Kiryu, Gunma 375-8515, Japan

Received 28 March 2007; accepted 10 May 2007
Available online 16 May 2007

Abstract

The effect of the pore structure and thickness of the porous carbon plate, PCP, as well as the gas barrier thickness on the methanol transport and the performance of a passive DMFC under the different cell voltages of 0.1, 0.2 and 0.3 V using different methanol concentrations was investigated. As a result of the mass transfer restrictions by employing the PCP, high methanol concentrations over 20 M could be efficiently used to produce the relatively high power density of 30 mW cm^{-2} for more than 10 h. The DMFC was operated under limiting current conditions in all the PCPs at 0.1 and 0.2 V to more than 20 M. The main factors for controlling the methanol transport were the barrier of the gas layer with CO_2, which was formed between the anode surface and the PCP and the properties of the PCP. At the low current densities of less than 60 mA cm^{-2}, when no CO_2 bubbles are emitted, both the pore structure and thickness of the PCP did not affect the methanol transport and the current voltage relationship. At the higher current densities, CO_2 bubbles were evolved through the PCP and different resistances to the methanol transport were observed depending on the PCP pore structure and thickness. The CO_2 gas layer between the MEA and the PCP caused a major resistivity for the methanol transport, and its resistivity increased with its thickness increasing. By using the PCP at 0.1 V, the energy density of the passive DMFC was significantly increased, e.g., more than seven times.

Keywords: Passive DMFC; Porous carbon plate; Pore structure; Barrier of the gas layer; Energy density

1. Introduction

There has been an increasing demand for the development of direct methanol fuel cells (DMFCs) because of their high theoretical energy densities that are suitable for mobile electric devices and automobiles. However, the energy density of the DMFCs currently under development is still far from that expected due to the methanol crossover and the high overvoltage at the electrodes [1–4]. Due to the methanol crossover, the DMFC usually shows the highest performance at the low concentrations of methanol from 2 to 3 M [5,6] under active conditions and about 5 M [7–9] under passive conditions. To overcome the methanol crossover, a large number of studies [10–14] were carried out for developing a new proton-conducting membrane with a low methanol permeability and high proton conductivity. Modification of the existing membranes like Nafion has also been conducted by conversion to a composite membrane [15–17] with inorganic or organic materials, surface modification by physical treatment [18] or by coating the surface with a thin film [7,19,20]. Only a few papers have considered reducing the ability for methanol crossover by mass transport control in the backing layer [21–26].

Lu et al. added a compact microporous layer to the backing structure as a barrier to the mass transport of methanol across the MEA. Thereby the rate of methanol crossover was reduced, but the maximum methanol concentration that can be used was as low as 8 M [21]. The authors have demonstrated, in recent reports [22–25], that a passive DMFC with a porous carbon plate, PCP, significantly reduced the methanol transport from the methanol reservoir to the anode surface. The separation of methanol through this type of passive DMFC under open circuit conditions was explained by diffusion control of the methanol transport by the PCP depending on the properties of the porous material, i.e., thickness, porosity and water absorptivity of the porous material. Under closed circuit conditions, the PCP and the CO_2 gas layer that formed between

* Corresponding author. Tel.: +81 277 30 1458; fax: +81 277 30 1457.
E-mail address: nakagawa@cee.gunma-u.ac.jp (N. Nakagawa).

0378-7753/$ – see front matter © 2007 Elsevier B.V. All rights reserved.
doi:10.1016/j.jpowsour.2007.05.015

the anode and the porous plate stably controlled the mass transport of methanol and water from the reservoir to the anode, and this facilitated operation with very high concentrations of methanol, even neat methanol. Recently, Guo and Faghri controlled the mass transport of methanol and water by storing them in hydrophobic and hydrophilic porous media, respectively, and they succeeded in using neat methanol, but with the addition of water from time to time, and they did not consider the effect of CO_2 under the closed circuit conditions on the mass transport of the solution [26]. Others have considered the control of the methanol transport from the reservoir to the anode surface via pervaporation membranes in which methanol was supplied in the gaseous phase [27].

In this study, we investigated the effect of the pore structure and thickness of the porous plate on the mass transport of methanol from the methanol reservoir to the anode surface under closed circuit conditions, and how these properties affect the cell performance and MCO. Also, the effect of the gas barrier thickness on the methanol transport and cell performance was investigated. We will discuss the mechanism for the restriction of the methanol transport in the case of a DMFC using a PCP.

2. Experimental

2.1. MEA preparation

The conventional MEA, which uses Pt and Pt–Ru black as the catalyst for the cathode and anode, respectively, was prepared and fabricated in the same manner as described in our previous reports [24,25]. The catalyst loading was 10–12 mg cm^{-2} in each electrode.

2.2. Porous carbon plates, PCP

The porous carbon plate, PCP, used for anode in this study was supplied from Mitsubishi Pencil Co. Ltd. The properties and pore structure of these porous carbon plates are listed in Table 1. The porous carbon plates were categorized into two types: the S type, PCPS, which was made of graphitic carbon and amorphous carbon and the Y type, PCPY, which was made of amorphous carbon. The microstructure of these porous plates was measured using a mercury porosimeter, (Pascal 140 + 440, Thermo Finnigan, Inc.). A perm-porometer (Porous Materials, Inc.) was used to measure the bubble point pressure, bubble pore diameter, using the Galwick solution with a surface tension of 15.7 dyne cm^{-1} and the resistivity of the two types of PCPs to airflow. Fig. 1 clearly showed that the resistivity for the airflow in the PCPS was greater than that of the PCPY type due to its smaller pore diameter. As shown in Table 1, PCPY had a larger pore diameter than that for the PCPS and the PCPY was used in two thicknesses, i.e., 1 mm for PCPY1 and 2 mm for PCPY2, to investigate the effect of the PCP thickness. The water absorptivities, as defined in our previous paper [23], of the different PCPs were measured and also shown in Table 1.

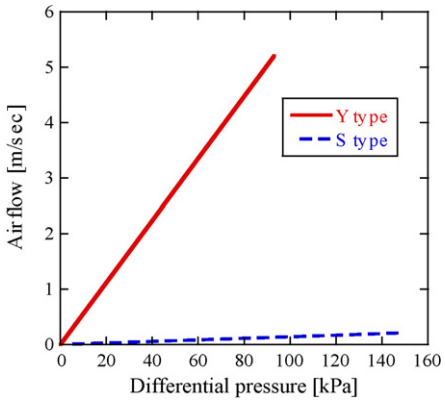

Fig. 1. Effect of PCP type on the airflow resistivity.

2.3. Passive DMFC with PCP

The MEA with the porous carbon plate was placed in a plastic holder as shown in Fig. 2. In the anode compartment, a 12 cm^3 methanol reservoir was prepared. The MEA was sandwiched between two current collectors, which were stainless steel plates of 2 mm thickness with open holes for the passages of fuel and oxidant. The open ratio of the area for the active electrode was 73%. The cell was arranged horizontally thus keeping the reser-

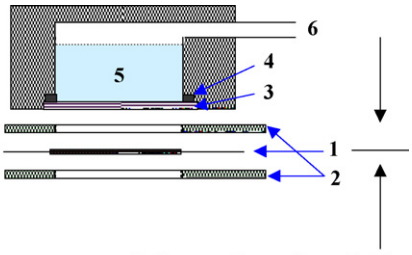

Fig. 2. Schematic diagram of passive DMFC with porous plate.

Table 1
Properties of the carbon plates used

PCP	δ (mm)	α_W (–)	Pore structure measured by the mercury porosimeter			By the perm-porometer	
			V_P ($cm^3\ g^{-1}$)	$d_{P,ave}$ (μm)	ε (–)	$P_{b.p.}$(kPa)	$d_{P,b.p.}$ (μm)
PCPY1	1.0	0.40	0.543	42.3	0.417	3.05	14.8
PCPY2	2.0	0.21					
PCPS1	1.0	0.15	0.556	1.425	0.457	42.76	1.05

δ, Thickness; α_W, water absorptivity; V_P, total cumulative volume; d_P, pore diameter; ε, total porosity; $P_{b.p.}$, bubble point pressure; $d_{P,b.p.}$, bubble point pore diameter.

voir upside to ensure constant contact between the solution and the PCP.

2.4. Operation with the gas barrier of different thicknesses

As a result of the configuration mentioned above, methanol had to pass through the porous plate then through the openings of the anode current collector. Under closed circuit conditions, the openings of the anode current collector were filled with CO_2 gas, which is enclosed between the porous plate and the anode. Therefore, a layer of CO_2 gas was formed between the porous plate and the anode and this gas layer obstructs methanol transport from the reservoir to the anode, methanol has to be transported through the gas layer as a vapor. To show the effect of the thickness of this gas barrier on the performance of the passive DMFC, different thickness of this gas barrier were prepared by changing the thickness of the anode current collector, i.e., 1, 2, 3 and 7 mm.

2.5. Measurement of the cell performance

In this study, all the experiments were conducted in the totally passive mode with the surrounding air at ambient conditions (293 K and 1 atm). A methanol solution, 6–7 cm^3, of different concentrations, from 2 M to neat methanol, was fed into the reservoir by a syringe through the open tube. We avoided direct contact of the MEA with the solution for a long time, when the methanol concentration was high. The current–voltage, *i–V*, characteristics were measured by linear sweep voltammetry from the OCV to zero at the scan rate of 1 mV s^{-1}. Thereafter, time versus the current density, i.e., the *i–t* characteristics, at the different cell voltages of 0.1, 0.2 and 0.3 V was measured from 5 to 12 h. These measurements were conducted using an electrochemical measurement system (HAG-5010, Hokuto Denko, Co. Ltd.). The temperature of the cell was also measured using a thermocouple placed between the surface of the anode current collector and the porous plate.

At the end of the *i–t* experiments for a certain methanol concentration, the weight loss of the entire cell holder was measured and the methanol concentration of the remained solution in the reservoir was also measured by gas chromatography. Based on the results, the methanol and water fluxes during the *i–t* experiment were calculated as shown below. The remaining solution was then removed from the reservoir, and a new solution with another concentration was injected into the cell. The same measurements were again conducted for the new solution.

2.6. Evaluation of the methanol, water fluxes and energy density

The average methanol and water fluxes during the *i–t* experiments were calculated on the basis of the weight loss and concentration change in the methanol solution before and after the *i–t* experiments as well as the amount of methanol and water that electrochemically reacted at the anode as described in our previous paper [24]. The methanol and water that reacted at the anode were calculated with the assumption that every molecule of methanol was completely converted to carbon dioxide producing six electrons and no intermediates. The Faraday efficiency for each concentration was calculated by dividing the reacted methanol at the anode by the total methanol loss during the *i–t* experiment [24].

The energy density was calculated on the basis of the volume of methanol solution input and completely consumed at the anode, evaluating the results from 2 M to a certain methanol concentration according to the following equation:

$$\text{Energy density} = \eta_f \eta_v \, \Delta G \, C_{max}$$

where (ΔG) Gibbs free energy of the oxidation reaction of methanol to produce CO_2 and water, 726 kJ mol^{-1}, (C_{max}) maximum methanol concentration that could be used at a certain cell voltage; (η_f) the average Faraday efficiencies of all methanol concentrations which could be used at a definite cell voltage; (η_v) voltage efficiency calculated by dividing the operating cell voltage, i.e., 0.1, 0.2 or 0.3 V, by the theoretical cell voltage of the DMFC, 1.18 V.

3. Results and discussion

3.1. Time versus current at different constant cell voltages

Fig. 3 shows the variations in the current density at 0.1 V for MEA/PCPS1 with different methanol concentrations that ranged from 4 to 22 M. The current density initially somewhat decreased and within few minutes, it became nearly constant with time. The difference between the initial and the nearly stable current density increased with the increasing methanol concentration, i.e., for 20 M, it was initially about 270 mA cm^{-2}, but decreased within 5 min to 170 mA cm^{-2}. The initial decrease in the current density would be caused by the initial methanol that accumulated at the anode surface under the open circuit conditions, where the PCP was left in contact with the methanol solution until saturation before any current flow, and during this time, a large MCO occurred and the cell temperature was initially high [24]. The value of the nearly stable current density increased with the increasing methanol concentration in which it increased from about 20 mA cm^{-2} at 4 M to about 170 mA cm^{-2}

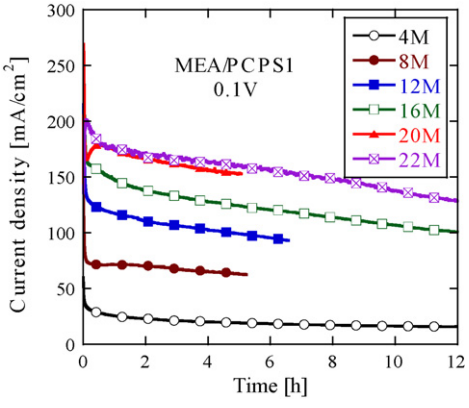

Fig. 3. Current profile during continuous operation of passive DMFC with PCPS1, MEA/PCPS1, at cell voltage of 0.1 V.

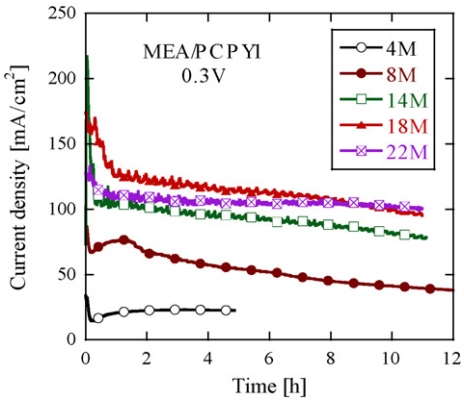

Fig. 4. Current profile during continuous operation of passive DMFC with PCPY1, MEA/PCPY1, at cell voltage of 0.3 V.

at 22 M. The current density was nearly constant with time due to the employment of the PCP, which constantly regulated the methanol transfer rate from the reservoir to the anode and prevented any excess loss of methanol by the MCO [24].

Fig. 4 shows the variations in current density at 0.3 V for MEA/PCPY1 for different methanol concentrations. The current density increased with the increasing methanol concentration up to 18 M, then decreased with a further increase in the methanol concentration. At 22 M, the initial performance was very high, showing about 60 mW cm^{-2}, but it decreased with time, and a constant power density around 30 mW cm^{-2} could be obtained. Fluctuations at a certain frequency in current density appeared at the high methanol concentrations of more than 14 M. The initial decrease in the current would be related to the same reasons shown above for the PCPS1, but it took longer time for the current density to be stable. This longer time should be due to the larger pore diameter of PCPY1, therefore, a lower resistivity to methanol transfer. The decrease in the current density with the increasing methanol concentration from 18 to 22 M would be caused by the high MCO at 22 M than at 18 M, as the dependency of MCO on the methanol concentration will be shown later. The fluctuations in the current could not be related to the flooding, because neither a water film nor water droplets were found in all of the experiments. These fluctuations may be related to the evolution of CO_2 bubbles from the porous plate, which in turn, will affect the methanol transfer across the PCP. This process periodically occurred, so fluctuations appeared in the current density.

3.2. *Effect of pore structure and thickness of PCP on current density and MCO at different cell voltages*

The different types of porous plates, PCPY1, PCPY2 and PCPS1, were used at the different cell voltages of 0.1, 0.2 and 0.3 V along with different methanol concentrations. In these experiments, the current density at 5 h from the start was defined as the stable current density, $i_{5\,h}$ and it was plotted at the different cell voltages versus the methanol concentration for the different PCPs, as shown in Figs. 5, 7 and 8.

Fig. 5 shows the effect of the pore structure and thickness of the PCP on the stable current density, $i_{5\,h}$, at 0.1 V. The stable

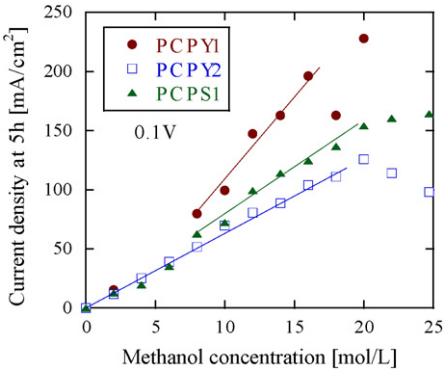

Fig. 5. Effect of pore structure and thickness of PCP on the stable current density, $i_{5\,h}$, at 0.1 V.

current density linearly increased with the increasing concentration up to 60 mA cm^{-2}, and there was no difference in the value of $i_{5\,h}$ for the different PCPs. On the other hand, above 60 mA cm^{-2}, every PCP had its own slope. The three PCPs were operated under limiting current conditions, which was clear from the linear dependency of $i_{5\,h}$ on the methanol concentration. The steeper slope of the line shows the lower rate of methanol transport. This regime verified that the rate of methanol transport was dependent on the current density, and the pore structure and thickness of the PCP.

Fig. 6 shows the effect of the pore structure and thickness of the PCP on the MCO during the *i–t* experiments shown in Fig. 5. The MCOs were similar to each other for the different PCPs in the low methanol concentration range, which showed similar current densities among them as shown in Fig. 5. Also, a higher MCO for PCPY1 compared to PCPY2 was obtained in the high methanol concentration range.

Under closed circuit conditions, the openings of the anode current collector were filled with CO_2 gas. Therefore, a layer of CO_2 gas was formed between the porous plate and the anode, and this gas layer obstructed the methanol transport and methanol diffused in the gaseous state from the reservoir to the anode surface. At the low current densities, no CO_2 bubbles come through the PCP as the CO_2 gas layer did not have a sufficient pressure to force the solution out from the pores of the PCP, and the CO_2 was transported by dissolving in the methanol solution through the

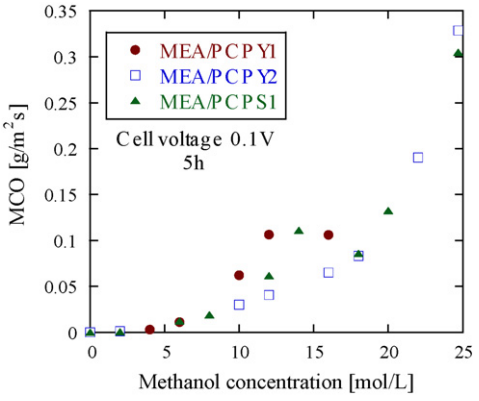

Fig. 6. Effect of pore structure and thickness of PCP on MCO at 0.1 V.

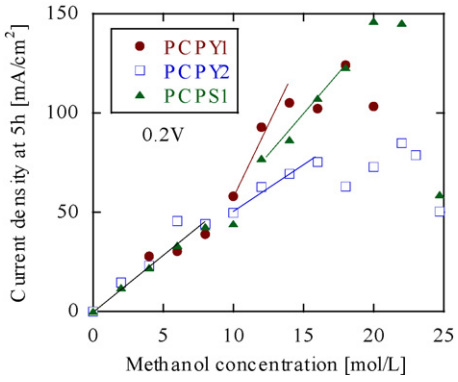

Fig. 7. Effect of pore structure and thickness of PCP on the stable current density, $i_{5\,h}$, at 0.2 V.

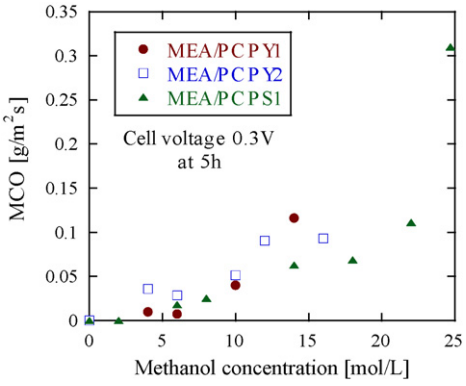

Fig. 9. Effect of PCP pore structure and thickness on MCO at 0.2 V.

PCP. The liquid/gas interface was found at the bottom surface of the PCP; therefore, the thickness of the gas layer was similar for each PCP along with a similar resistivity for the methanol transport. The resistance of the PCP with this gas layer was very high in comparison with the PCP alone; therefore, there was no clear difference between the different types of PCPs in this range. However, as the current density increased, the pressure of the gas layer increased and the surface tension of the methanol solution decreased due to the increase in the methanol concentration. Therefore, CO_2 bubbles could push the solution out from some pores of the PCP and escape out through the PCP. At this point, the pressure of the CO_2 gas layer in the barrier instantaneously decreased. This may induce some solution to enter through pores instead of the gas out. This situation would be largely dependent on the properties of the PCP, where the gas easily escaped through thinner plates with a large pore diameter than through thicker plates with a small pore diameter, and this situation, in turn, would affect the resistivity of the gas layer. PCPY1 had a large pore diameter, small thickness and low bubble point pressure, so it showed the lowest resistivity for the gas removal. Therefore, the higher methanol transport for PCPY1 would cause the steep slope of the line at high current densities as shown in Fig. 5. On the other hand, PCPY2 and PCPS1 had higher resistivities due to the significant thickness or the small pore diameter, respectively; therefore, both of them would maintain a high resistivity to methanol transport across the PCP based on their gentle slopes of the lines as shown in Fig. 5.

Fig. 7 shows the effect of the pore structure and thickness of the PCP on the stable current density, $i_{5\,h}$, at 0.2 V. A similar behavior as that shown in Fig. 5 was obtained, but with lower current density values, where $i_{5\,h}$ linearly increased with the increasing concentration up to 60 mA cm^{-2}, and all of the PCPs had a similar slopes. However, this slope was different among all the PCPs at the higher current densities. At this cell voltage, 0.2 V, the three PCPs still operated under limiting current conditions, which was clear from the linear dependency of $i_{5\,h}$ on the methanol concentration, but with smaller current density values than that for 0.1 V. For the same reasons discussed for Fig. 5,

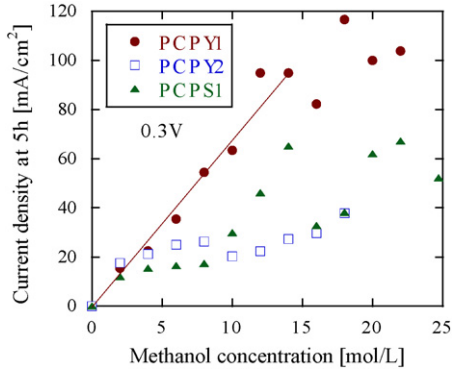

Fig. 8. Effect of pore structure and thickness of PCP on the stable current density, $i_{5\,h}$, at 0.3 V.

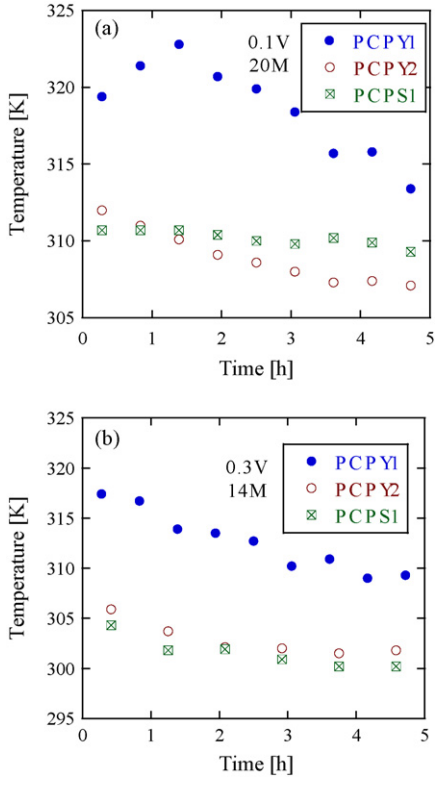

Fig. 10. Variations in operating cell temperature of passive DMFC with different porous plates during *i–t* measurements: (a) at 0.1 V and 20 M and (b) at 0.3 V and 14 M.

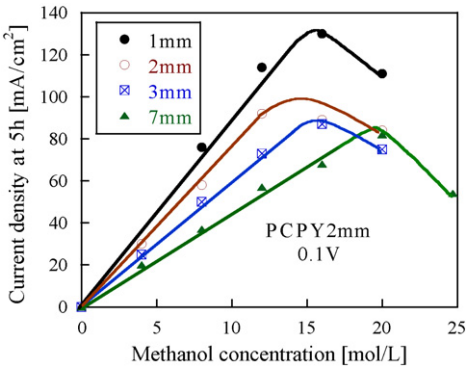

Fig. 11. Effect of gas layer thickness on the stable current density, $i_{5\,h}$, using PCPY2 at 0.1 V.

the pore structure and thickness of the PCP did not affect the performance in the low current density range, but affected it at the higher current densities above 60 mA cm^{-2}.

Fig. 8 shows the effect of the pore structure and thickness of the PCP on the stable current density, $i_{5\,h}$, at 0.3 V. In this figure, it was clear that a linear relationship between $i_{5\,h}$ and methanol concentration appeared only for PCPY1 up to 12 M. This suggested that the operation under limiting current still appeared for PCPY1, but not for PCPY2 and PCPS1. This would result from the different activities of the electrodes for each MEA. Although the MCO for PCPY1 was high, the reactivity of the electrodes for PCPY1 was high, which showed a linear relationship.

Fig. 9 shows the effect of the pore structure and thickness of the PCP on the MCO during the *i–t* experiments shown in Fig. 8. No clear difference in the MCO among the different types of PCPs was found although a higher MCO for PCPY1 was postulated.

Fig. 10a and b shows the temperature profile during the *i–t* experiments at 0.1 and 0.3 V for the different types of PCPs, respectively. At 14 and 20 M, the cell temperatures for PCPY2 and PCPS1 were nearly the same and lower than that for PCPY1 by about 10 °C. The increase in cell temperature for PCPY1 than that for PCPY2 and PCPS1 would be related to the MCO, which was higher in the case of PCPY1 than that for the other two PCPs.

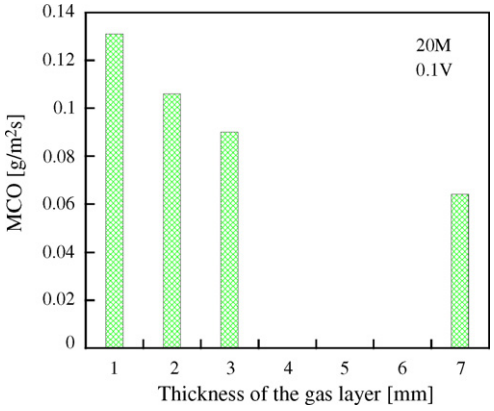

Fig. 12. Effect of gas layer thickness on MCO at 0.1 V.

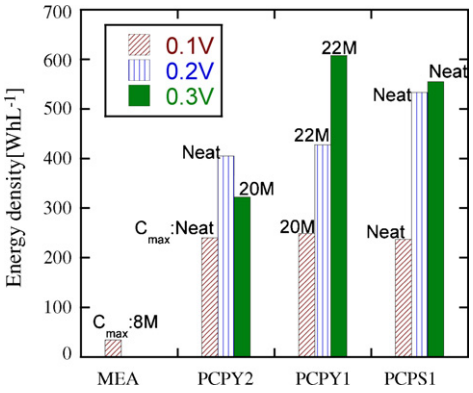

Fig. 13. Effect of PCP pore structure and thickness on the energy density of passive DMFC at different cell voltages.

3.3. Effect of the thickness of the gas layer on current density and MCO

Fig. 11shows the effect of the thickness of the gas layer between the PCP and the anode on the stable current density. With the increasing methanol concentration, the stable current density increased up to 130 mA cm^{-2} for a 1 mm thickness at 16 M and up to 80 mA cm^{-2} for a 7 mm thickness at 20 M. Up to 16 M, the $i_{5\,h}$ decreased with the increasing barrier thickness from 1 to 7 mm. The reduction in $i_{5\,h}$ with the increasing thickness of the gas barrier would be due to the increase in the resistivity of the gas layer.

Fig. 12 shows the effect of the gas barrier thickness on the average MCO during the *i–t* experiments using PCPY2 at 0.1 V and 20 M. The MCO decreased from 1.31 to 0.064 g m^{-2} s^{-1} with the increasing gas barrier thickness from 1 to 7 mm. The reduction in the MCO with the increasing gas barrier thickness was due to the increased resistivity to methanol transport across this gas layer.

3.4. Effect of PCP pore structure and thickness on energy density

Fig. 13 shows the effect of the PCP pore structure and thickness on the energy density at the different cell voltages of 0.1, 0.2 and 0.3 V as well as that of the conventional MEA at 0.1 V. The energy density largely increased as a result of using the PCP. It increased more than seven times when compared to that without the PCP. The increase in the energy density for the PCP would result from controlling the MCO by the PCP; therefore, the Faraday efficiency increased as well as voltage efficiency by working at a high cell voltage. The energy density was the highest for the PCPS1 and PCPY1 at 0.3 V, and this was caused by the high cell efficiency for PCPS1 and PCPY1 due to good control of the MCO or high cell temperature, respectively.

4. Conclusions

The effects of the pore structure and thickness of the PCP as well as the gas layer thickness on the mass transfer and performance of a passive DMFC at the different cell voltages of 0.1,

0.2 and 0.3 V using different methanol concentrations ranging from 2 M to neat methanol were investigated, and the following conclusions were obtained.

(1) As a result of the mass transfer restrictions by employing the PCP, high methanol concentrations could be used that efficiently produced a relatively high constant power density of 30 mW cm^{-2} for PCPY1 at 0.3 V and 22 M for more than 10 h.
(2) The thickness of the gas layer, which was formed between the PCP and the anode surface, was one of the most important factors in limiting methanol transport. The effect of the PCP structure and thickness on the cell performance appeared at the relatively high current densities.
(3) It was demonstrated that using the PCP is quite effective for achieving a high energy density for passive DMFCs, and a higher resistance to methanol transport across the gas barrier could be obtained by increasing its thickness.

Acknowledgement

The authors acknowledge Mitsubishi Pencil Co. Ltd., for the preparation and gift of the porous carbon plates.

References

[1] A.S. Arico, S. Srinivasan, V. Antonucci, Fuel Cells 1 (2001) 133–161.
[2] T. Schultz, S. Zhou, K. Sundmacher, Chem. Eng. Technol. 24 (2001) 1223–1233.
[3] J.G. Liu, T.S. Zhao, R. Chen, C.W. Wong, Electrochem. Commun. 7 (2005) 288.
[4] J.G. Liu, T.S. Zhao, Z.X. Liang, R. Chen, J. Power Sources 153 (2006) 61–67.
[5] S. Surampudi, S.R. Narayanan, E. Vamos, H. Frank, G. Halpert, A. LaConti, J. Kosek, G.K. Surya Prakash, G.A. Olah, J. Power Sources 47 (1994) 377–385.
[6] M.K. Ravikumar, A.K. Shukla, J. Electrochem. Soc. 143 (1996) 2601–2606.
[7] S.R. Yoon, G.H. Hwang, W.I. Cho, I.-H. Oh, S.-A. Hong, H.Y. Ha, J. Power Sources 106 (2002) 215–223.
[8] R. Chen, T.S. Zhao, J. Power Sources 152 (2005) 122–130.
[9] B. Bae, B.K. Kho, T. Lim, I. Oh, S. Hong, H.Y. Ha, J. Power Sources 158 (2006) 1256–12261.
[10] J.T. Wang, S. Wasmus, R.F. Savinell, J. Electrochem. Soc. 143 (1996) 1233–1239.
[11] E. Peled, T. Duvdevani, A. Aharon, A. Melman, Electrochem. Solid State Lett. 3 (2000) 525–528.
[12] M.V. Fedkin, X. Zhou, M.A. Hofmann, E. Chalkova, J.A. Weston, H.R. Allcock, S.N. Lvov, Mater. Lett. 52 (2002) 192–196.
[13] T. Yamaguchi, M. Ibe, B.N. Nair, S. Nakao, J. Electrochem. Soc. 149 (2002) A1448–A1453.
[14] M.L. Ponce, L. Prado, B. Ruffmann, K. Richau, R. Mohr, S.P. Nunes, J. Membr. Sci. 217 (2003) 5–15.
[15] A.S. Arico, P. Creti, P.L. Antonucci, V. Antonucci, Electrochem. Solid State Lett. 1 (1998) 66–68.
[16] C. Yang, S. Srinivasan, A.S. Arico, P. Creti, V. Baglio, V. Antonucci, Electrochem. Solid State Lett. 4 (2001) A31–A34.
[17] N. Jia, M.C. Lefevre, J. Halfyard, S. Qi, P.G. Pickup, Electrochem. Solid State Lett. 3 (2000) 529–531.
[18] I.J. Hobson, H. Ozu, M. Yamaguchi, M. Muramatsu, S. Hayase, J. Mater. Chem. 12 (2002) 1650–1656.
[19] W.C. Choi, J.D. Kim, S.I. Woo, J. Power Sources 96 (2001) 411–414.
[20] Y.K. Xiu, K. Kamata, T. Ono, K. Kobayashi, T. Nakazato, N. Nakagawa, Electrochemistry 73 (2005) 67–70.
[21] G.Q. Lu, C.Y. Wang, T.J. Yen, X. Zhang, Electrochim. Acta 49 (2004) 821.
[22] N. Nakagawa, K. Kamata, A. Nakazawa, M. Ali Abdelkareem, K. Sekimoto, Electrochemistry 74 (3) (2006) 221–225.
[23] N. Nakagawa, M. Ali Abdelkareem, K. Sekimoto, J. Power Sources 160 (2006) 105–115.
[24] M. Ali Abdelkareem, N. Nakagawa, J. Power Sources 162 (2006) 114–123.
[25] M. Ali Abdelkareem, N. Nakagawa, J. Power Sources 165 (2007) 685–691.
[26] Z. Guo, A. Faghri, J. Power Sources 160 (2006) 1142–1155.
[27] H. Kim, J. Power Sources 162 (2006) 1232–1235.